Propagation inhibition and wave localization in a two-dimensional random liquid medium

Yu-Yu Chen and Zhen Ye
Wave Phenomena Laboratory, Department of Physics, National Central University, Chung-li, Taiwan 320, Republic of China
(Received 7 September 2001; published 15 May 2002)

Acoustic propagation and scattering in water containing many parallel air-filled cylinders is studied in an exact manner. Two situations are considered and compared; (1) wave propagating through the array of cylinders, imitating common experimental setups, and (2) wave transmitted from a source located inside the ensemble. We show that waves can be blocked from propagation by disorders in the first scenario, but such an inhibition does not necessarily lead to actual wave localization in the medium. The results indicate that the traditional method may be ambiguous in discerning localization effects. Furthermore, the results reveal the phenomenon of wave localization in a range of frequencies.

DOI: 10.1103/PhysRevE.65.056612 PACS number(s): 43.20.+g, 42.25.Fx

I. INTRODUCTION

When propagating through media containing many scatterers, waves will be repeatedly scattered by each scatterer, forming a multiple scattering process [1]. Multiple scattering of waves is responsible for many fascinating phenomena, such as random laser [2], electronic transport in impure solids [3], and photonic or acoustic band gaps [4–6]. Under proper conditions, multiple scattering leads to the unusual phenomenon of wave localization. That is, waves in a randomly scattered medium are trapped in space and will remain confined around the initial transmitting site until dissipated.

Over the past 20 years, tremendous efforts have been devoted to the investigation of the localization phenomenon of classical waves in random media (e.g., Refs. [7–14]). Observation of classical wave localization is a difficult task, partially because suitable systems are hard to find and partially because observation is often complicated by such effects as absorption and attenuation, leading to much debate [12,13].

Another difficulty with previous observations may be associated with the method that the localization is investigated. As stated in Ref. [12], to date, claims of localization have been based on observations of the exponential decay of waves as they propagate *through* disordered media. That is, in most previous experimental studies, the apparatus is set up in such a way that waves are transmitted at one end of a scattering ensemble, then the scattered waves are recorded on the other end to measure the transmission through the sample. The results are subsequently compared with the previous theory to infer possible localization effects. As will be shown in this paper, we find that such a traditional method has ambiguities in isolating localization effects [15].

The purpose of this paper is twofold. First, we would like to point out that previous experimental methods have uncertainties in discerning localization effects, as the observation can be obscured by effects such as reflection and deflection. These effects attenuate waves, resulting in a similar decay in transmission and thus making the data interpretation ambiguous. We show that while wave localization does lead to an inhibition in wave propagation, the propagation inhibition does not necessarily imply wave localization. In other words, it is necessary to differentiate the situation that waves are blocked from transmission from the situation that waves can be actually localized in the medium. Second, we show that in the system we study, waves are not always localized for all frequencies in conflict with the previous prediction. Wave localization is evident in a range of frequencies and when there is a sufficient density of random scatterers.

The paper is structured as follows. In the following section, we present the model system and the necessary formulation solving the multiple scattering of waves in the system. The results and discussion are presented in Sec. III, followed by a brief summary in Sec. IV.

II. FORMULATION AND SYSTEM SETUP

The model in this paper is acoustic propagation in water containing many parallel air-filled cylinders. Different from the common approach that derives approximately a diffusion equation for the ensemble-averaged energy, our method is to solve the wave propagation from the fundamental wave equation, without resorting to approximations. The model has been studied previously for the coherent behavior of acoustic propagation [16] and the acoustic complete band gaps [17].

Consider N straight cylinders located at $\vec{r}_i$ with $i=1,2,\ldots,N$ to form either a completely random or regular array. An acoustic line source transmitting monochromatic waves is placed at $\vec{r}_s$. The scattered wave from each cylinder is a response to the total incident wave composed of the direct wave from the source and the multiply scattered waves from other cylinders. The final wave reaching a receiver located at $\vec{r}_r$ is the sum of the direct wave from the source and the scattered waves from all the cylinders. Such a scattering problem can be solved *exactly*, following Twersky [18]. While the details are in Ref. [19], the essential procedures are summarized below.

The scattered wave from the jth cylinder can be written as

$$p_s(\vec{r},\vec{r}_j)=\sum_{n=-\infty}^{\infty} i\pi A_n^j H_n^{(1)}(k|\vec{r}-\vec{r}_j|)e^{in\phi_{\vec{r}-\vec{r}_j}}, \qquad (1)$$

where k is the wave number of the medium, $H_n^{(1)}$ is the

nth-order Hankel function of the first kind, and $\phi_{\vec{r}-\vec{r}_j}$ is the azimuthal angle of the vector $\vec{r}-\vec{r}_i$ relative to the positive x axis.

The total wave incident around the ith scatterer $p^i_{in}(\vec{r})$ is a superposition of the direct contribution from the source $p_0(\vec{r})=G(\vec{r}-\vec{r}_s)=i\pi H_0^{(1)}(k|\vec{r}-\vec{r}_s|)$ and the scattered waves from all other scatterers:

$$p^i_{in}(\vec{r})=p_0(\vec{r})+\sum_{j=1,j\neq i}^{N} p_s(\vec{r},\vec{r}_j). \tag{2}$$

In order to separate the governing equations into modes, we can express the total incident wave in term of the modes about $\vec{r}_i$:

$$p^i_{in}(\vec{r})=\sum_{n=-\infty}^{\infty} B^i_n J_n(k|\vec{r}-\vec{r}_i|)e^{in\phi_{\vec{r}-\vec{r}_i}}. \tag{3}$$

The expansion is in terms of Bessel functions of the first kind J_n to ensure that $p^i_{in}(\vec{r})$ does not diverge as $\vec{r}\to\vec{r}_i$. The coefficients B^i_n are related to the A^j_n in Eq. (1) through Eq. (2). A particular B^i_n represents the strength of the nth mode of the total incident wave on the i-th scatterer with respect to the ith scatterer's coordinate system (i.e. around $\vec{r}_i$). In order to isolate this mode on the right hand side of Eq. (2), and thus determine a particular B^i_n in terms of the set of A^j_n, we need to express $p_s(\vec{r},\vec{r}_j)$, for each $j\neq i$, in terms of the modes with respect to the ith scatterer. In other words, we want $p_s(\vec{r},\vec{r}_j)$ in the form

$$p_s(\vec{r},\vec{r}_j)=\sum_{n=-\infty}^{\infty} C^{j,i}_n J_n(k|\vec{r}-\vec{r}_i|)e^{i\phi_{\vec{r}-\vec{r}_i}}. \tag{4}$$

This can be acheived (i.e. $C^{j,i}_n$ expressed in terms of A^i_n) through the following addition theorem [20]:

$$H_n^{(1)}(k|\vec{r}-\vec{r}_j|)e^{in\phi_{\vec{r}-\vec{r}_j}}=e^{in\phi_{\vec{r}_i-\vec{r}_j}}\sum_{l=-\infty}^{\infty} H^{(1)}_{n-l}(k|\vec{r}_i-\vec{r}_j|) \times e^{-il\phi_{\vec{r}_i-\vec{r}_j}}J_l(k|\vec{r}-\vec{r}_i|)e^{il\phi_{\vec{r}-\vec{r}_i}}. \tag{5}$$

Taking Eq. (5) into Eq. (1), we have

$$p_s(\vec{r},\vec{r}_j)=\sum_{n=-\infty}^{\infty} i\pi A^j_n e^{in\phi_{\vec{r}_i-\vec{r}_j}}\sum_{l=-\infty}^{\infty} H^{(1)}_{n-l}(k|\vec{r}_i-\vec{r}_j|) \times e^{-il\phi_{\vec{r}_i-\vec{r}_j}}J_l(k|\vec{r}-\vec{r}_i|)e^{il\phi_{\vec{r}-\vec{r}_i}}. \tag{6}$$

Comparing with Eq. (4), we see that

$$C^{j,i}_n=\sum_{l=-\infty}^{\infty} i\pi A^j_l H^{(1)}_{l-n}(k|\vec{r}_i-\vec{r}_j|)\exp[i(l-n)\phi_{\vec{r}_i-\vec{r}_j}]. \tag{7}$$

Now we can relate B^i_n to $C^{j,i}_n$ (and thus to A^j_l) through Eq. (2). First note that through the addition theorem the source wave can be written,

$$\begin{aligned} p_0(\vec{r}) &= i\pi H_0^{(1)}(kr) \\ &= i\pi\sum_{l=-\infty}^{\infty} H^{(1)}_{-l}(k|\vec{r}_i|)e^{-il\phi_{\vec{r}_i}}J_l(k|\vec{r}-\vec{r}_i|)e^{il\phi_{\vec{r}-\vec{r}_i}} \\ &= \sum_{l=-\infty}^{\infty} S^i_l J_l(k|\vec{r}-\vec{r}_i|)e^{il\phi_{\vec{r}-\vec{r}_i}}, \end{aligned} \tag{8}$$

where

$$S^i_l=i\pi H^{(1)}_{-l}(k|\vec{r}_i|)e^{-il\phi_{\vec{r}_i}}. \tag{9}$$

Matching coefficients in Eq. (2) and using Eqs. (3), (4), and (8), we have

$$B^i_n=S^i_n+\sum_{j=1,j\neq i}^{N} C^{j,i}_n. \tag{10}$$

At this stage, S^i_n are known, but both B^i_n and A^j_l are unknown. Boundary conditions will give another equation relating them.

The boundary conditions are that the pressure and the normal velocity should be continuous across the interface between a scatterer and the surrounding medium. The total wave outside the ith scatterer is $p_{ext}=p^i_{in}(\vec{r})+p_s(\vec{r},\vec{r}_i)$. The wave inside the ith scatterer can be expressed as

$$p^i_{int}(\vec{r})=\sum_{n=-\infty}^{\infty} D^i_n J_n(k^i_1|\vec{r}-\vec{r}_i|)e^{in\phi_{\vec{r}-\vec{r}_i}}. \tag{11}$$

The boundary conditions are then

$$p_{ext}|_{\partial\Omega^i}=p_{int}|_{\partial\Omega^i} \tag{12}$$

and

$$\frac{1}{\rho}\frac{\partial p_{ext}}{\partial n}\bigg|_{\partial\Omega^i}=\frac{1}{\rho^i_1}\frac{\partial p_{int}}{\partial n}\bigg|_{\partial\Omega^i}, \tag{13}$$

where $\partial\Omega^i$ is the boundary of the ith scatterer, k and ρ are the wave number and density of the surrounding medium, and k^i_1 and ρ^i_1 are the wave number and density of the ith scatterer, respectively. Using Eqs. (1), (3), and (11), multiplying both sides of the boundary condition equations by $e^{in\phi_{\vec{r}-\vec{r}_i}}$, and integrating over the boundary $\partial\Omega^i$, we have for the case of circular cylindrical scatterers,

$$B^i_n J_n(ka^i)+i\pi A^i_n H^{(1)}_n(ka^i)=D^i_n J_n(ka^i/h^i), \tag{14}$$

$$B^i_n J'_n(ka^i)+i\pi A^i_n H^{(1)'}_n(ka^i)=\frac{1}{g^i h^i}D^i_n J'_n(ka^i/h^i). \tag{15}$$

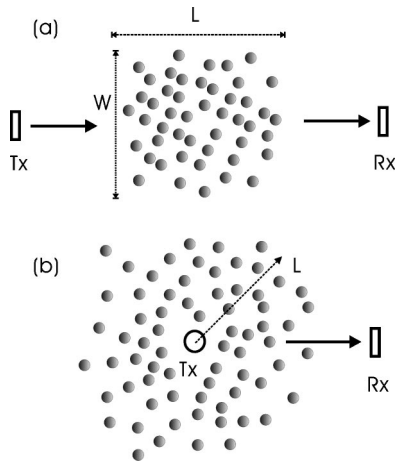

FIG. 1. Conceptual layout: (a) acoustic propagation through a cloud of cylinders; (b) acoustic transmission from a line source located inside a cylinder cloud.

Here a^i is the radius of the ith cylinder, $g^i=\rho_1^i/\rho$ is the density ratio, and $h^i=k/k_1^i=c_1^i/c$ is the sound speed ratio for the ith cylinder. Elimination of D_n^i gives

$$B_n^i = i\pi\Gamma_n^i A_n^i, \tag{16}$$

where

$$\Gamma_n^i = \left[\frac{H_n^{(1)}(ka^i)J_n'(ka^i/h^i) - g^i h^i H_n^{(1)'}(ka^i)J_n(ka^i/h^i)}{g^i h^i J_n'(ka^i)J_n(ka^i/h^i) - J_n(ka^i)J_n'(ka^i/h^i)}\right]. \tag{17}$$

If we define

$$T_n^i = S_n^i/i\pi = H_{-n}^{(1)}(k|\vec{r}_i|)e^{-in\phi_{\vec{r}_i}} \tag{18}$$

and

$$G_{l,n}^{i,j} = H_{l-n}^{(1)}(k|\vec{r}_i-\vec{r}_j|)\exp[i(l-n)\phi_{\vec{r}_i-\vec{r}_j}], \quad i\neq j, \tag{19}$$

then Eq. (10) becomes

$$\Gamma_n^i A_n^i - \sum_{j=1,j\neq i}^{N}\sum_{l=-\infty}^{\infty} G_{l,n}^{i,j}A_l^j = T_n^i. \tag{20}$$

If the value of n is limited to some finite range, then this is a matrix equation for the coefficients A_n^i. Once solved, the total wave at any point outside all cylinders is

$$p(\vec{r}) = p_0(\vec{r}) + \sum_{i=1}^{N}\sum_{n=-\infty}^{\infty} i\pi A_n^i H_n^{(1)}(k|\vec{r}-\vec{r}_i|)e^{in\phi_{\vec{r}-\vec{r}_i}}. \tag{21}$$

The acoustic intensity is represented by the squared module of the transmitted wave. The normalized transmission is defined as $T\equiv p/p_0$.

We must stress that total wave expressed by Eq. (21) incorporates all orders of multiple scattering. We also emphasize that the above derivation is valid for any configuration of the cylinders. In other words, Eq. (21) works for situations where the cylinders can be placed either randomly or in order. For a regular array of the cylinders, band structures for the wave propagation appear. They can be readily computed by the standard plane-wave method [6].

III. RESULTS AND DISCUSSION

In the following computation, we assume N uniform air cylinders of radius a. The fraction of area occupied by the cylinders per unit area is β. The average distance between nearest neighbors is, therefore, $d=(\pi/\beta)^{1/2}a$, which is also the lattice constant for the corresponding square lattice array. Two situations are considered; (1) wave propagating through the array of cylinders, labeled hereafter as the ''outside'' situation that imitates the traditional experimental setup, and (2) wave transmitted from a source located inside the ensemble, labeled hereafter as the ''inside'' situation. Both cases are illustrated in Fig. 1. For the outside case, all cylinders are randomly or regularly placed within a rectangular area with length L and width W. The transmitter and receiver are located at some distance from the two opposite sides of the scattering area. For the inside situation, all cylinders are placed completely randomly or regularly within a circle of radius L with the transmitting source located at the center and the receiver located outside the scattering cloud. In the

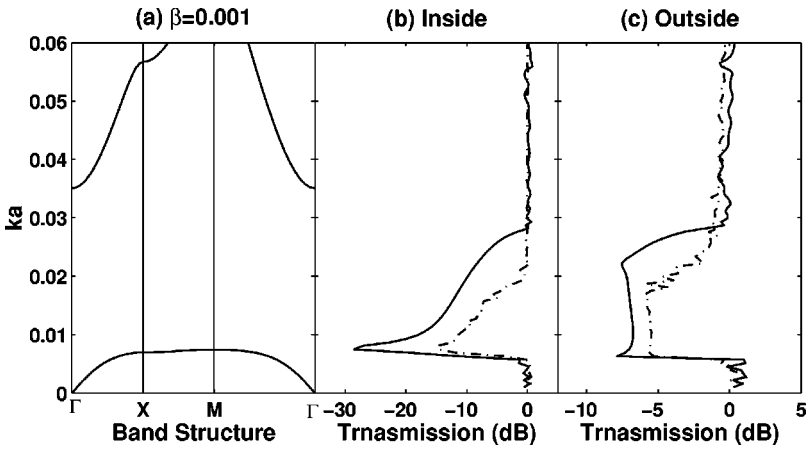

FIG. 2. The middle and right panels, referring to the inside and outside cases, respectively, show the normalized acoustic transmission versus frequency in terms of nondimensional ka. Here the comparison is made between the results from the corresponding square arrays (solid lines) and from the complete random array of cylinders (dotted lines). Left panel: The band structures computed by the plane-wave expansion method.

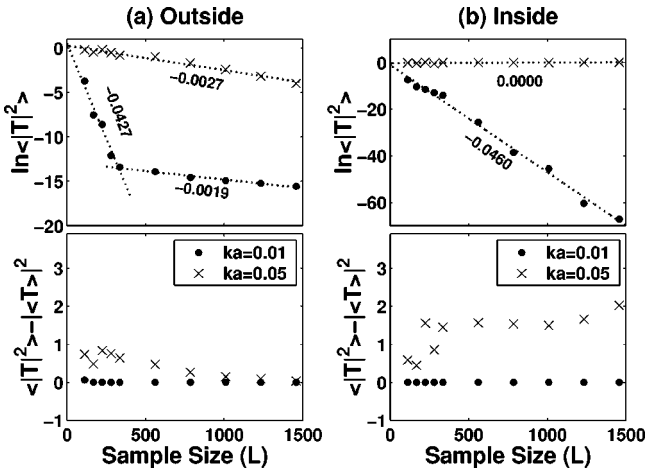

FIG. 3. Normalized acoustic transmission and its fluctuation versus the sample size for two frequencies. The left and right panels refer to the inside and outside cases, respectively. The estimated slopes for the transmission are indicated in the figure. Here $T \equiv p/p_0$.

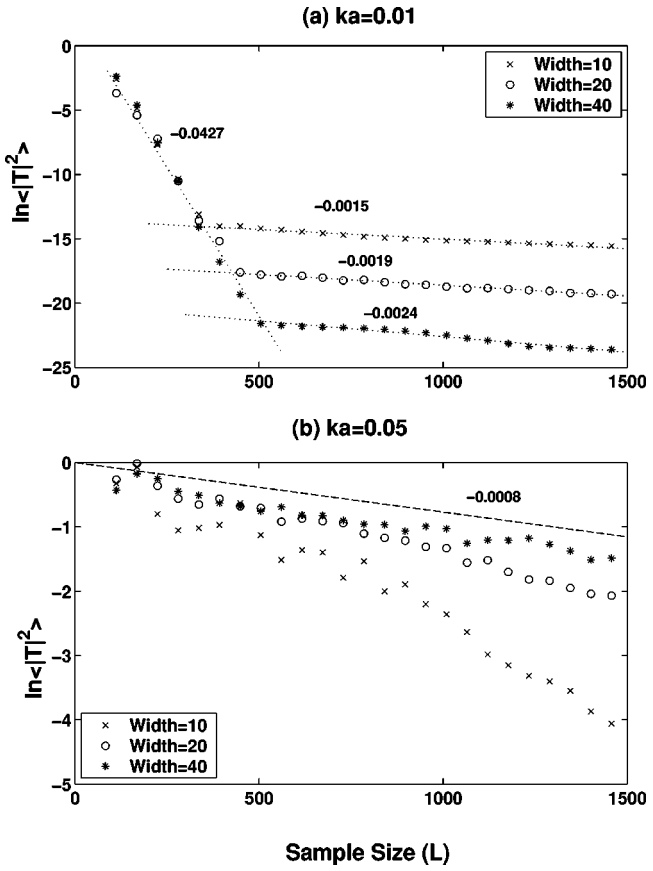

FIG. 4. Normalized total acoustic transmission across a scattering array as a function of the sample length for different sample widths. The solid line in (b) is the numerical extrapolation as the width approaches infinity.

computation, the acoustic intensity is normalized in such a way that its value equals unity when there are no scatterers present; thus the uninteresting geometrical spreading effect is naturally eliminated. We scale all lengths by the parameter d, and the frequency in terms of nondimensional ka; in this way, the computation becomes nondimensional.

A set of numerical computations has been performed for various area fractions β, numbers N, and dimensionless frequency ka. The major controlling parameter is β. The transmitter and receiver are placed at a distance of $2d$ from the sample; in fact, we found that as long as we keep the symmetry the results remain qualitatively unchanged as the positions of transmitter and receiver vary. Though it is the line source that is used in computation, the features hold even when a beamed cylindrical plane wave is used.

Figure 2 presents typical results for the transmitted intensity as a function of ka for the two situations in Fig. 1, with $\beta=10^{-3}$ and $N=200$. For reference, we also plot the band structure, following Refs. [6,17], and the transmission for each corresponding square lattice with the same β. Here it is shown that for both situations, there is a significant transmission reduction regime from $ka=0.007$ to about 0.022, which is roughly coincident with the complete band gap shown by Fig. 2(a), and within this regime, the transmission is less inhibited compared to that from the corresponding square lattice arrays. For the inside case, the reduction regime for the random scattering is identified as the localization range. This reduction regime will be widened as β increases, but will disappear when β drops below about 10^{-5}. Comparing the results from the random arrays and that from the corresponding square lattice arrays, a significant difference is apparent: outside the severe reduction regime, the transmission is reduced by the randomization in the outside case, for example, at $ka=0.05$, but stays nearly unchanged in the inside scenario. More explicitly, the randomness tends to block the wave propagation outside the gap regime. Previously, such propagation inhibition caused by randomness has been regarded as the indication of wave localization. In what follows, we show that waves are actually not localized at these frequencies.

We consider two frequencies as an example, $ka=0.01$ and 0.05. Figure 3 presents the results for the random ensemble-averaged transmission and its fluctuation as a function of the sample size at the two frequencies for the fixed $\beta=10^{-3}$. For the outside case, the width of the sample is fixed at $W=20$. The sample size is varied by adjusting the number of the cylinders. A few important features are discovered.

For $ka=0.01$, the transmission decays exponentially with the sample size for both inside and outside situations. In the outside case, there are two decay slopes, i.e., $-0.042\,7$ and $-0.001\,9$. There is a transition regime separating the two slopes. The transmission starts to decay with slope $-0.042\,7$, followed by a milder decay of slope -0.0019. The slope of $-0.042\,7$ is nearly the same as the decay slope of $-0.046\,0$ in the inside case. Obviously, this is because at $ka=0.01$, waves are localized. This exponential decay actually indicates that waves are trapped or localized near the transmitting source; this is clearly shown by the top portion of Fig. 3(b). The second slope in the outside case for $ka=0.01$ is due to the finite width of the sample, as will be

discussed later. Inside the localization regime, the transmission fluctuation is small, as expected from an earlier work [16]. Here we see that within the localization regime, wave localization can be observed in both outside and inside scenarios.

For $ka=0.05$, the inside and outside scenarios differ significantly. While for the outside case the transmission decreases exponentially with a slope of 0.002 7 along the path, the transmission in the inside situation does not decrease. For the outside case, the transmission fluctuation increases then drops along the path, emulating the localization effect. For the inside case, however, the transmission fluctuation representing the diffusive intensity [1] increases as more and more scattering occurs along the path, fully complying with the well-known nonlocalized Milne diffusion. The large fluctuation implies that the transmission is sensitive to the distribution of the cylinders, which is another indication of the nonlocalization property [16]. In fact, the apparent decay in the outside case is due to the scattering attenuation that the waves are reflected and scattered away from the forward direction. These results suggest that waves are actually not localized for $ka=0.05$, and it would be a mistake to interpret the exponential decay shown in the outside situation as the indication of wave localization.

Now we consider the width effect in the outside situation. In Fig. 4, the ensemble-averaged total transmission is plotted as a function of the sample size (L) for three widths (W) at two frequencies.

For frequencies inside the localization regime, the second slope is due to the finite width, and can be interpreted as follows. At $ka=0.01$, the localization effect is dominant, thus leading to a rapid decay in transmission along the path, giving rise to the first slope. As expected, this slope is almost independent of the width. As the sample size increases, the directly transmitted waves are almost completely blocked. But, due to the finite width, a small amount of the deflected waves around the sample sides can still reach the receiver. When increasing the sample size (L) for a fixed width (W), this effect gradually diminishes along the path, yielding the second slope. Increasing width (W) will reduce this finite-width effect, and thus the amount of deflected waves reaching the receiver will also decrease, as shown. The width effect disappears when the width approaches infinity. For $ka=0.05$, outside the localization regime, the transmission decays nearly exponentially along the path. As the width increases, the slope will become smaller, and will be saturated to a value of -0.0008. These results indicate that in the outside scenario, the path-dependent transmission behaves similarly for frequencies either inside or outside the localization regime as long as the width is sufficiently large; therefore, the phenomenon of wave localization cannot be isolated in this scenario.

IV. CONCLUDING REMARKS

In summary, we have pointed out that current experimental methods have uncertainties in discerning localization effects. This also partially explains why in the past the observation of localization effects has *not* been conclusive and has led to so much debate (e.g., Refs. [12,13]). In order to isolate the phenomenon of wave localization without ambiguity, new experimental approaches are desirable. Finally, we restress that whether waves are localized or extended is an intrinsic property of the system that is supposed to be infinite. This property does not depend on the source, and should not depend on boundaries either. While the source is placed inside the medium with increasing sizes, the infinite system can be mimicked and the localization property could be probed without ambiguity.

ACKNOWLEDGMENT

The work received support from National Science Council of Republic of China.

[1] A. Ishimaru, *Wave Propagation and Scattering in Random Media* (Academic Press, New York, 1978).
[2] N.M. Lawandy, R.M. Balachandran, A.S.L. Gomes, and E. Sauvain, Nature (London) **368**, 436 (1994); H. Cao *et al.*, Phys. Rev. Lett. **82**, 2278 (1999).
[3] P.W. Anderson, Phys. Rev. **109**, 1492 (1958).
[4] See, e. g., E. Yablonovitch, Phys. Rev. Lett. **58**, 2059 (1987); S. John, *ibid.* **58**, 2486 (1987); W. Robertson *et al.*, *ibid.* **68**, 2023 (1992).
[5] J.V. Sánchez-Pérez *et al.*, Phys. Rev. Lett. **80**, 5325 (1998).
[6] M.S. Kushwaha, Int. J. Mod. Phys. B **10**, 977 (1996).
[7] T.R. Kirkpatrick, Phys. Rev. B **31**, 5746 (1985).
[8] A.Z. Genack and N. Garcia, Phys. Rev. Lett. **66**, 2064 (1991).
[9] R. Dalichaouch, J.P. Amstrong, S. Schultz, P.M. Platzman, and S.L. McCall, Nature (London) **354**, 53 (1991); A.Z. Genack and N. Garcia, Phys. Rev. Lett. **66**, 2064 (1991).
[10] A. Lagendijk and B.A. van Tiggelen, Phys. Rep. **270**, 143 (1996).
[11] M. van Albada and A. Lagendijk, Phys. Rev. Lett. **55**, 2692 (1985); P.E. Wolf and G. Maret, *ibid.* **55**, 2696 (1985).
[12] A.A. Chabanov, M. Stytchev, and A.Z. Genack, Nature (London) **404**, 850 (2000).
[13] See, e. g., F. Scheffold, R. Lenke, R. Tweer, and G. Maret, Nature (London) **398**, 206 (1999); D.S. Wiersma, P. Bartolini, A. Lagendijk, and R. Roghini, *ibid.* **398**, 207 (1999).
[14] D.S. Wiersma, P. Bartolini, A. Lagendijk, and R. Roghini, Nature (London) **390**, 671 (1997).
[15] E. Abrahams, P.W. Anderson, D.C. Licciardello, and T.V. Ramakrishnan, Phys. Rev. Lett. **42**, 673 (1979).
[16] E. Hoskinson and Z. Ye, Phys. Rev. Lett. **83**, 2734 (1999).
[17] Z. Ye and E. Hoskinson, Appl. Phys. Lett. **77**, 4428 (2000).
[18] V. Twersky, J. Acoust. Soc. Am. **24**, 42 (1951).
[19] Y.-Y. Chen and Z. Ye, Phys. Rev. E **64**, 036616 (2001).
[20] I. S Gradshteyn, I. M. Ryzhik, and A. Jeffrey, *Table of Integrals, Series, and Products*, 5th ed. (Academic Press, New York, 1994).